

*Supporting information*

**Enhanced Drug Loading in Polymerized Micellar Cargo**

*Julien Ogier,<sup>a</sup> Thomas Arnauld,<sup>\*c</sup> Géraldine Carrot,<sup>b</sup> Antoine Lhumeau,<sup>c</sup> Jean-Marie Delbos,<sup>c</sup> Claire Boursier,<sup>c</sup> Olivier Loreau,<sup>a</sup> Francois Lefoulon,<sup>c</sup> Eric Doris<sup>\*a</sup>*

a) CEA, iBiTecS, Service de Chimie Bioorganique et de Marquage, 91191 Gif-sur-Yvette, France,  
b) Technologie Servier, 27 rue Eugène Vignat, 45000 Orléans, France,  
c) CEA, Laboratoire Léon Brillouin, 91191 Gif-sur-Yvette, France.

- Nanostructures derived from diacetylenic amphiphile <b>1</b>	S2
- NMR spectra of photo-polymerizable amphiphile <b>1</b>	S3
- Synthesis of <sup>14</sup> C- amphiphile <b>10</b>	S4
- Determination of the CMC of photo-polymerizable amphiphile <b>1</b>	S6
- Drug loading experiments	S7
- Tissue distribution of total radioactivity in the male wistar rat after single intravenous administration of <sup>14</sup> C-polymerised micelles	S9
- Quantitative tissue distribution of total radioactivity in the male C56 black mouse after single intravenous infusion of various formulations of <sup>14</sup> C-CPTD-1	S15

Nanostructures derived from diacetylenic amphiphile 1

At lower pH (~ 7), polymerized amphiphile **1** forms well defined ribbons (Figure 1a-b) which evolve to tubular nanostructures (Figure 1c-d) when heated above 70°C. At pH above 12, micelles are formed (Figure 1e-f).

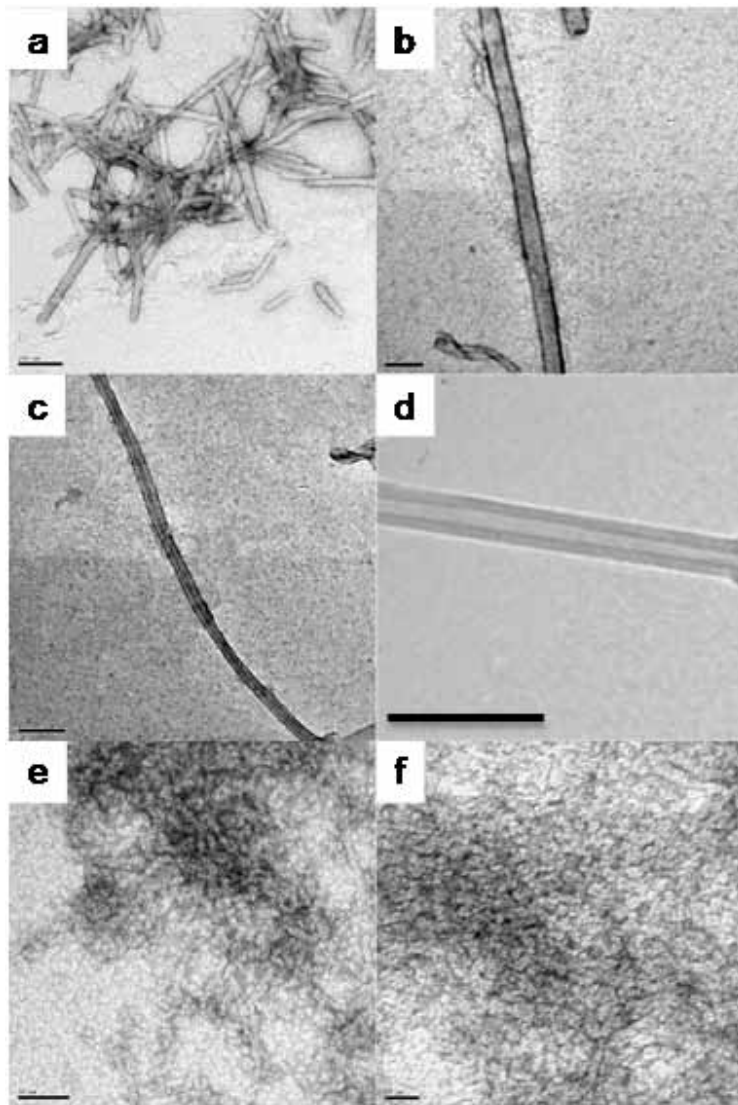


**Figure S1** – Structure of polymerized amphiphile **1** in: (S1a-b) ribbon (pH 7) (S1c-d) nanotube (pH 7 and heated at 70°C) (S1e-f) micelles (pH=12)

Scale bars : (S1a) 200 nm (S1b) 50 nm (S1c) 100 nm (S1d) 50 nm (S1e) 50 nm (S1f) 20 nm.

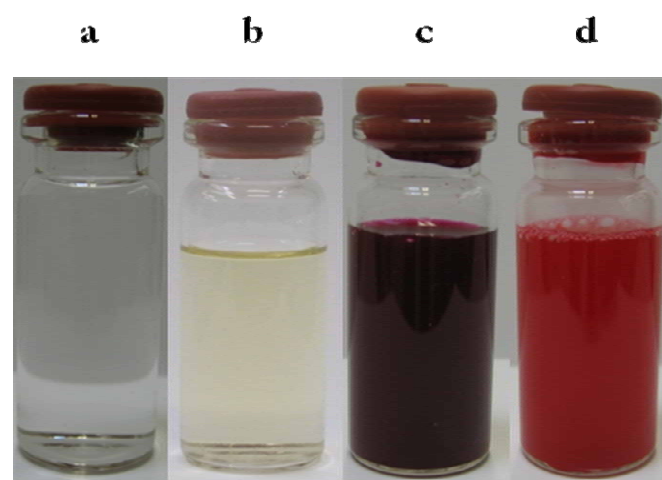


**Figure S2.** Pictures of solutions of (a) non-polymerized micelles, (b) polymerized micelles, (c) ribbons, and (d) coiled ribbons.

NMR spectra of photo-polymerizable amphiphile 1

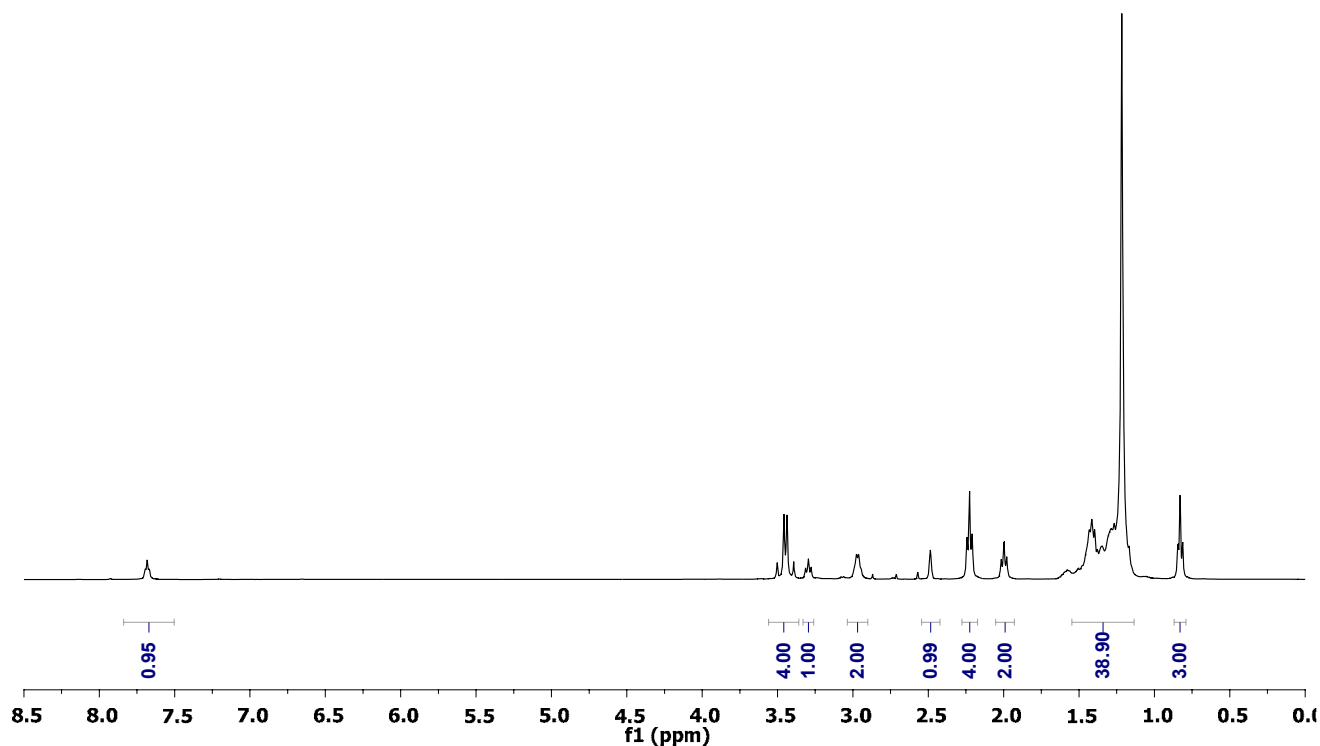


**Figure S3.** <sup>1</sup>H NMR of photo-polymerizable amphiphile 1 in DMSO-d<sub>6</sub>

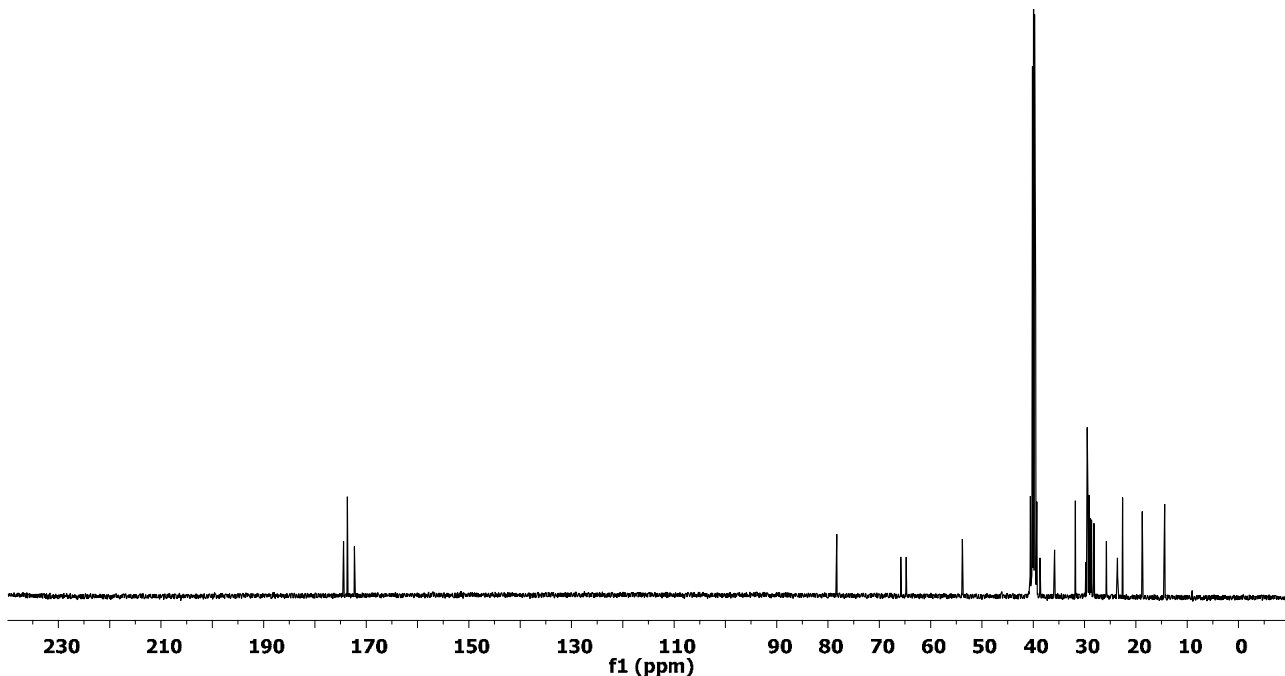


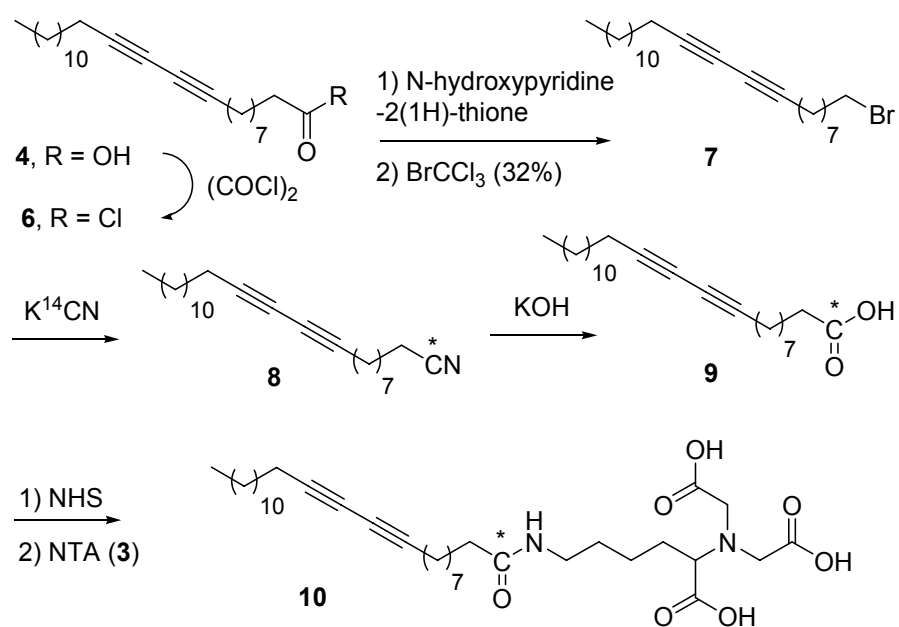
**Figure S4.**  $^{13}\text{C}$  NMR of photo-polymerizable amphiphile **1** in  $\text{DMSO-d}_6$

Synthesis of  $^{14}\text{C}$ - amphiphile **10** (Scheme S1).

*1-Bromotetracosa-9,11-diyne (7).* 10,12-pentacosadiynoic acid **4** (1 g, 2.67 mmol, 1 equiv.) was solubilized in 10 mL of toluene and oxalyl chloride (1.1 mL, 5 equiv.) was added dropwise at 0 °C. The resulting solution was stirred at r.t. under  $\text{N}_2$  for 12 hrs and concentrated under vacuum. The residue was taken back into toluene and evaporated to remove traces of oxalyl chloride (this operation was repeated 3 times). The resulting acid chloride **6** was used in the next step without further purification. DMAP (126 mg, 0.4 equiv.) and 2-mercaptopuridine *N*-oxide sodium salt (478 mg, 1.2 equiv.) were solubilized in 15 mL of  $\text{BrCCl}_3$ . The solution was heated to reflux and acid chloride **6**, in 5 mL of  $\text{BrCCl}_3$ , was added. The mixture was refluxed for an additional hour. The solution was diluted with 50 mL of  $\text{Et}_2\text{O}$  and washed 3 times with sat NaCl. The organic layer was dried over  $\text{MgSO}_4$ , filtered, and concentrated. Purification by column chromatography over  $\text{SiO}_2$  (pentane) gave 349 mg of 1-bromotetracosa-9,11-diyne **7**. Yield: 32%.  $^1\text{H}$  NMR ( $\text{CDCl}_3$ ): 3.4 (t,  $J=6.8$  Hz, 2H), 2.24 (t,  $J=6.8$  Hz, 4H), 1.85 (m, 2H), 1.2-1.6 (m, 30H), 0.89 (t,  $J=6.8$  Hz, 3H).  $^{13}\text{C}$  NMR ( $\text{CDCl}_3$ ): 78.2 (2C), 65.2 (2C), 33.9 (1C), 32.7 (1C), 31.8 (1C), 26.7-29.6 (13C), 22.6 (1C), 19.1 (2C), 14.1 (1C).

[*1-<sup>14</sup>C]-10,12-Pentacosadiynoic acid (**9**)}. Bromo derivative **7** (82.1 mg, 201 µmol, 1 equiv.) and K<sup>14</sup>CN (36.2 mg, 2.7 equiv., 27 mCi, specific activity: 53 mCi/mmol) were solubilized in 10 mL of DMSO. The solution was stirred overnight at 80°C under Ar. The solution was then diluted with 20 mL of Et<sub>2</sub>O and 30 mL of H<sub>2</sub>O were added. The aqueous phase was extracted two times with Et<sub>2</sub>O. The organic phases were collected, dried over MgSO<sub>4</sub>, filtered and concentrated. Purification by column chromatography over SiO<sub>2</sub> (pentane/Et<sub>2</sub>O: 90/10) gave <sup>14</sup>C-labeled nitrile **8** (160 µmol, 8.5 mCi). Compound **8** was solubilized in 10mL of EtOH and 10 mL of 40% aqueous KOH was added. The solution was heated to 80°C for 6 hrs. The solution was cooled to r.t. and 10% HCl was added until pH 1 is reached. The aqueous phase was extracted three times with Et<sub>2</sub>O. The organic phases were collected, dried over MgSO<sub>4</sub>, filtered and concentrated. Purification by column chromatography over SiO<sub>2</sub> (hexane/EtOAc/AcOH: 85/15/0.1) gave labeled carboxylic acid **9** (50 mg, 133 µmol, 7 mCi). Yield from **7**: 66%. Liquid scintillation counting: 140 µCi/mg. Radiochemical purity: 94.3%.*

*N<sub>2</sub>-(bis-carboxymethyl)-N<sub>6</sub>-[*1-<sup>14</sup>C]-pentacosa-10,12-diynoyl-Lysine (**10**)*. Under Ar, [*1-<sup>14</sup>C*] carboxylic acid **9** (25 mg, 66 µmol, 3.5 mCi, 1 equiv.) and pentacosa-10,12-diynoic acid **4** (225 mg, 9 equiv.) were solubilized in 25 mL of anhydrous CH<sub>2</sub>Cl<sub>2</sub>. To this solution were added *N*-hydroxysuccinimide (116 mg, 1.5 equiv.) and EDC (195 mg, 1.5 equiv.). The solution was stirred at r.t. for 12 hrs. The organic phase was washed twice with H<sub>2</sub>O, dried over MgSO<sub>4</sub>, filtered and concentrated under vacuum to give the corresponding activated carboxylic acid (312 mg, 664 µmol) as a pale pink solid. The latter was diluted with 10 mL of DMF before being added to a mixture of 6-amino-2(bis-carboxymethyl-amino)-hexanoic acid **3** (230 mg, 1.3 equiv.) in 30 mL of DMF, 2 mL of H<sub>2</sub>O, and 1 mL of NEt<sub>3</sub>. The solution was stirred at room temperature for 12 hrs. The solution was concentrated, taken back into 30 mL of H<sub>2</sub>O and slowly acidified to pH 1 with 1N HCl. The precipitate was centrifuged and washed 2 times with 1N HCl. The orange solid was then dried overnight under vacuum and over P<sub>2</sub>O<sub>5</sub>. Yield: quant. Liquid scintillation counting: 7.6 µCi/mg. Radiochemical purity: 91.0%. NMR <sup>1</sup>H (d<sub>6</sub>-DMSO): 7.68 (t, J=5.6 Hz, 1H), 3.50 (AB, 4H, J<sub>AB</sub>=17.6 Hz), 3.35 (t, J=7.3 Hz, 1H), 2.97 (m, 2H), 2.24 (t, J=6.8 Hz, 4H), 2.00 (t, J=7.2 Hz, 2H), 1.1-1.6 (m, 38H), 0.83 (t, J=6.8 Hz, 3H). MS (ESI/TOF) m/z: (ESI<sup>+</sup>) 617 (100), 618 (26.3), 619 (5.2).*



**Scheme S1.** Synthesis of <sup>14</sup>C- amphiphile **10**

Determination of the Critical Micelle Concentration of photo-polymerizable amphiphile 1

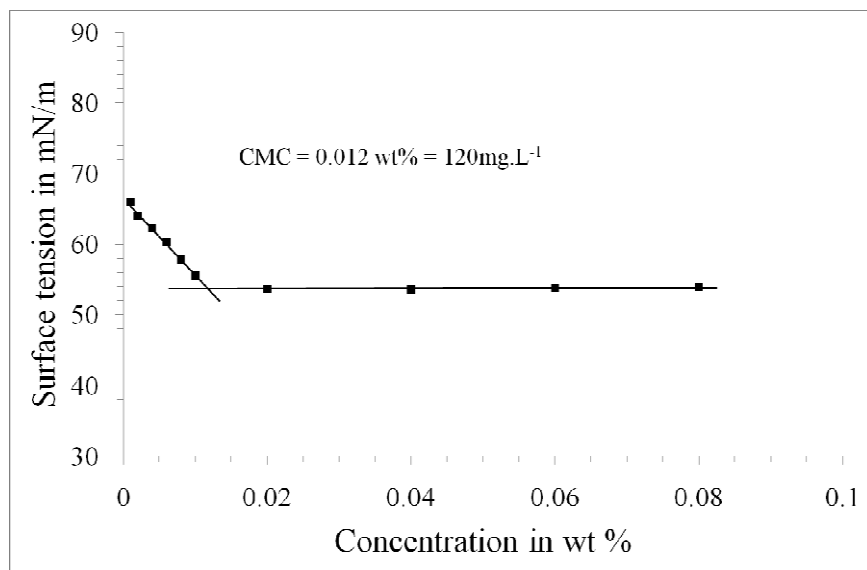


**Figure S5-** Measurement of the CMC of photo-polymerizable amphiphile **1** by the ring method

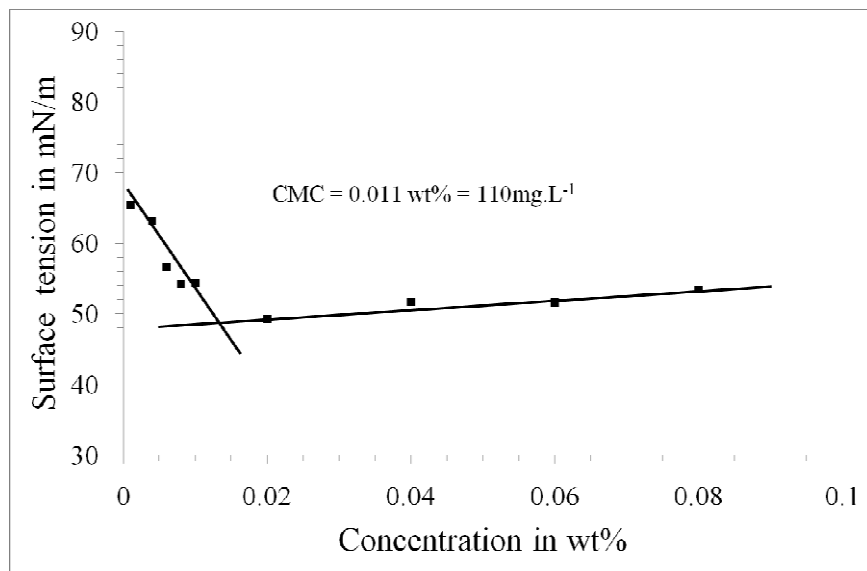


**Figure S6-** Measurement of the CMC photo-polymerizable amphiphile **1** by the plate method

### Drug loading experiments

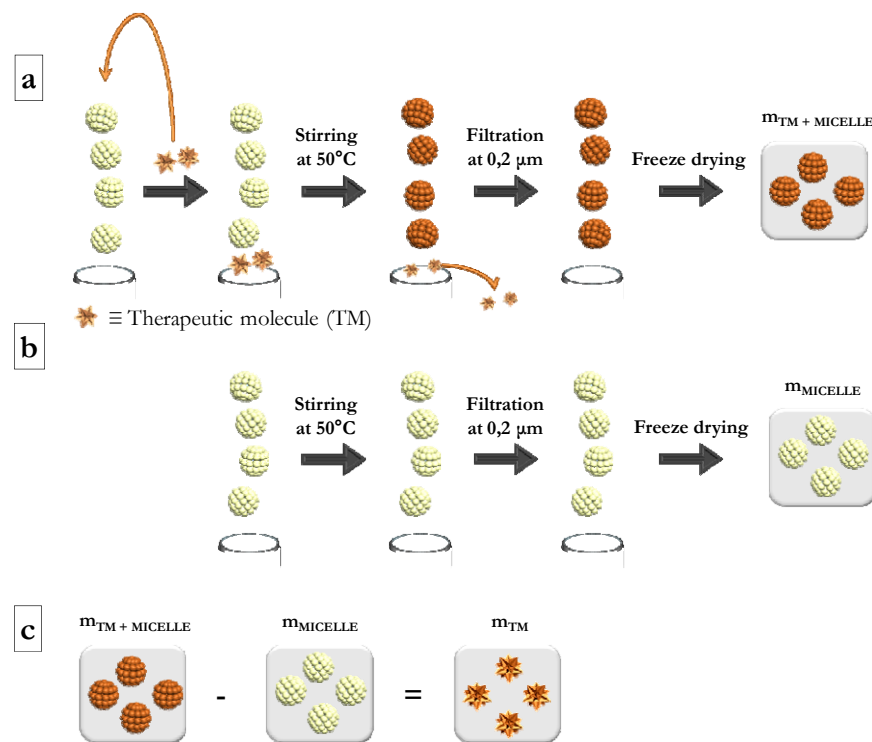


**Figure S7** – Determination of the drug loading by mass balance: (a) inclusion of TM at 50°C (b) blank experiment (c) weight of solubilized TM determined by mass balance of the two experiments (a) and (b).

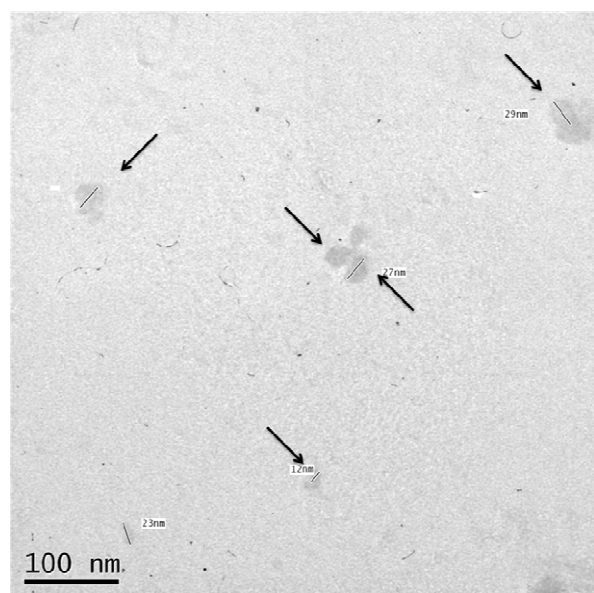


**Figure S8** – TEM pictures of FLD loaded in polymerized micelles

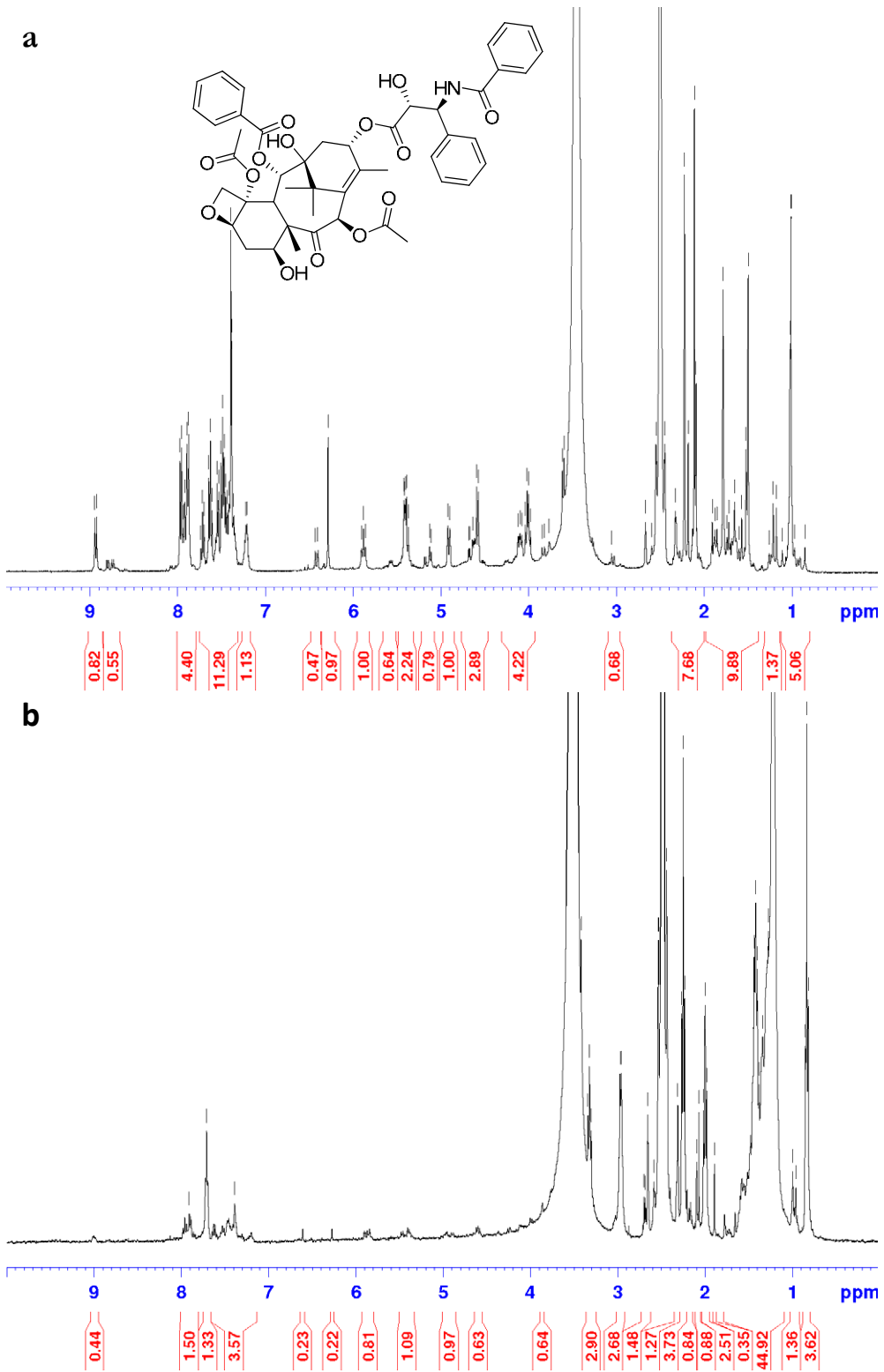


**Figure S9 –  $^1\text{H}$  NMR spectra of (a) Paclitaxel in  $\text{DMSO-d}_6/\text{DCl}$ , (b) Paclitaxel/micelle complex in  $\text{DMSO-d}_6/\text{DCl}$**

Tissue distribution of total radioactivity in the male wistar rat after single intravenous administration of [<sup>14</sup>C]-polymerised micelles

*Species/Strain/Gender:* Rat/Wistar/Male

*Method of administration/volume (mL/kg):* intravenous bolus/ 2.5

*Sampling times:* 0.17 and 24

*Radionuclide:* <sup>14</sup>C

*Compounds/batches:* <sup>14</sup>C-polymerised micelles

*Doses (MBq/kg – mg/kg):* 4 – 100

*Specific activity (MBq/ mg of total compound in formulation):* .0365

*Radiochemical purity (%):* 100 in stock solution

*Formulation:* physiological saline (0.9 g/L NaCl)

*Analyte:* Total radioactivity <sup>14</sup>C

*Samples:* Sagittal sections of each rat (at 10 min or 24h after dosing) and urine samples collected at 24h (rat 2) after dosing

*Analytical methods:* Radioluminography to quantify radioactive levels in tissues and liquid scintillation counting to measure radioactivity in urine.

**TABLE S1:** Tissue distribution of total radioactivity versus time after single intravenous administration of 4 MBq/kg [<sup>14</sup>C]-polymerised micelles and polymerised micelles (100 mg/kg) in male Wistar rats.  
Expressed in Bq/g

Time (h)	0.17	24
<b>Tissues/organs</b>		
ADRENAL GLANDS	35644	12224
BLOOD	50303	2275
BONE MARROW	22006	8605
BONE MINERAL	600	466
BRAIN	997	234
BROWN FAT	14783	2994
FAT	903	729
HEART	21137	2859
INTESTINE WALL	9052	14591
KIDNEY CORTEX	22465	11907
KIDNEY CORTICOMEDULLA	22789	4446
KIDNEY MEDULLA	37148	2358
LACHRYMAL GLAND	5282	4667
LIVER	36547	20639
LUNG	45005	5079
OESOPHAGUS WALL	1649	
PANCREAS	11422	4669
PITUITARY GLAND	9385	6271
PROSTATE		
SALIVARY GLANDS	8335	4387
SEMINAL VESICLES	128	1679
SKELETAL MUSCLE	2015	574
SKIN	2521	1491
SPINAL CORD	1212	480
SPLEEN	31053	14098
STOMACH WALL	2420	1285
TESTIS	1291	1504
THYMUS	3590	3533
THYROID GLAND	12428	2579
URINARY BLADDER WALL		
UVEAL TRACT	5264	1968

**TABLE S2:** Tissue distribution of total radioactivity versus time after single intravenous administration of 4 MBq/kg [<sup>14</sup>C]-polymerised micelles and polymerised micelles (100 mg/kg) in male Wistar rats.  
Expressed in ng eq/g

Tissues/organs	Time (h)	0.17	24
<b>ADRENAL GLANDS</b>		976662	335424
<b>BLOOD</b>		1378326	62415
<b>BONE MARROW</b>		602966	236122
<b>BONE MINERAL</b>		16440	12777
<b>BRAIN</b>		27309	6412
<b>BROWN FAT</b>		405061	82152
<b>FAT</b>		24752	20003
<b>HEART</b>		579155	78439
<b>INTESTINE WALL</b>		248029	400354
<b>KIDNEY CORTEX</b>		615561	326707
<b>KIDNEY CORTICOMEDULLA</b>		624420	121985
<b>KIDNEY MEDULLA</b>		1017863	64701
<b>LACHRYMAL GLAND</b>		144720	128067
<b>LIVER</b>		1001396	566305
<b>LUNG</b>		1233149	139354
<b>OESOPHAGUS WALL</b>		45183	
<b>PANCREAS</b>		312959	128113
<b>PITUITARY GLAND</b>		257163	172070
<b>PROSTATE</b>			
<b>SALIVARY GLANDS</b>			
<b>SEMINAL VESICLES</b>		3516	46070
<b>SKELETAL MUSCLE</b>		55221	15750
<b>SKIN</b>		69067	40912
<b>SPINAL CORD</b>		33209	13180
<b>SPLEEN</b>		850858	386845
<b>STOMACH WALL</b>		66309	35250
<b>TESTIS</b>		35365	41277
<b>THYMUS</b>		98359	96942
<b>THYROID GLAND</b>		340542	70756
<b>URINARY BLADDER WALL</b>			
<b>UVEAL TRACT</b>		144236	54000

**TABLE S3:** Tissue distribution of total radioactivity versus time after single intravenous administration of 4 MBq/kg [<sup>14</sup>C]-polymerised micelles and polymerised micelles (100 mg/kg) in male Wistar rats.  
 Expressed in % dose/g

Tissues/organs	Time (h)	0.17	24	t <sub>1/2</sub> (2 pts) (h)
<b>ADRENAL GLANDS</b>		4.17	1.44	15.5
<b>BLOOD</b>		5.89	0.268	5.35
<b>BONE MARROW</b>		2.58	1.01	17.7
<b>BONE MINERAL</b>		0.0703	0.0549	67.0
<b>BRAIN</b>		0.117	0.0276	11.5
<b>BROWN FAT</b>		1.73	0.353	10.4
<b>FAT</b>		0.106	0.0860	79.8
<b>HEART</b>		2.48	0.337	8.29
<b>INTESTINE WALL</b>		1.06	1.72	NC
<b>KIDNEY CORTEX</b>		2.63	1.40	26.3
<b>KIDNEY CORTICOMEDULLA</b>		2.67	0.524	10.2
<b>KIDNEY MEDULLA</b>		4.35	0.278	6.01
<b>LACHRYMAL GLAND</b>		0.618	0.550	142
<b>LIVER</b>		4.28	2.43	29.3
<b>LUNG</b>		5.27	0.599	7.60
<b>OESOPHAGUS WALL</b>		0.193		NC
<b>PANCREAS</b>		1.34	0.551	18.6
<b>PITUITARY GLAND</b>		1.10	0.740	41.7
<b>PROSTATE</b>				NC
<b>SALIVARY GLANDS</b>		0.976	0.517	26.0
<b>SEMINAL VESICLES</b>		0.0150	0.198	NC
<b>SKELETAL MUSCLE</b>		0.238	0.0677	13.2
<b>SKIN</b>		0.295	0.176	31.9
<b>SPINAL CORD</b>		0.142	0.0566	18.0
<b>SPLEEN</b>		3.64	1.66	21.1
<b>STOMACH WALL</b>		0.283	0.152	26.4
<b>TESTIS</b>		0.151	0.177	NC
<b>THYMUS</b>		0.420	0.417	1865
<b>THYROID GLAND</b>		1.46	0.304	10.6
<b>URINARY BLADDER WALL</b>				NC
<b>UVEAL TRACT</b>		0.616	0.232	16.9

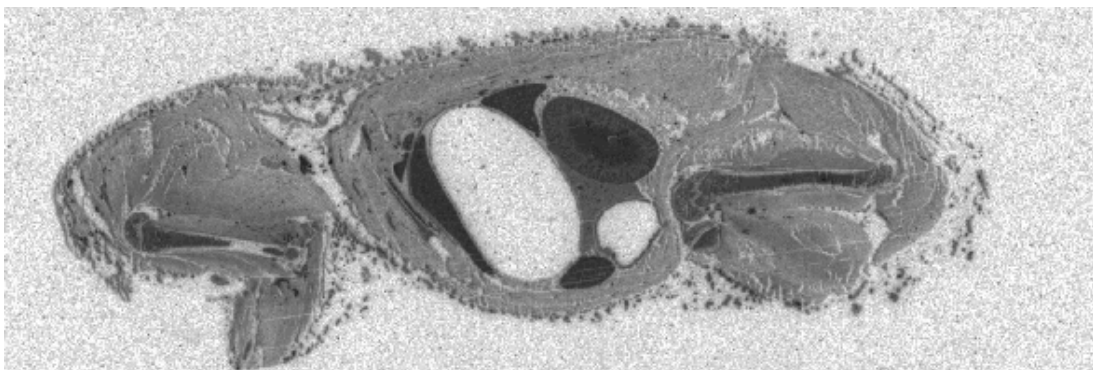
NC: not calculated

**TABLE S4:** Tissue distribution of total radioactivity versus time after single intravenous administration of 4 MBq/kg [<sup>14</sup>C]-polymerised micelles and polymerised micelles (100 mg/kg) in male Wistar rats.

Tissue/blood ratios

Tissues/organs	Time (h)	0.17	24
<b>ADRENAL GLANDS</b>		0.709	5.37
<b>BLOOD</b>		1	1
<b>BONE MARROW</b>		0.437	3.78
<b>BONE MINERAL</b>		0.0119	0.205
<b>BRAIN</b>		0.0200	0.103
<b>BROWN FAT</b>		0.294	1.32
<b>FAT</b>		0.0180	0.320
<b>HEART</b>		0.420	1.26
<b>INTESTINE WALL</b>		0.180	6.41
<b>KIDNEY CORTEX</b>		0.447	5.23
<b>KIDNEY CORTICOMEDULLA</b>		0.453	1.95
<b>KIDNEY MEDULLA</b>		0.738	1.04
<b>LACHRYMAL GLAND</b>		0.105	2.05
<b>LIVER</b>		0.727	9.07
<b>LUNG</b>		0.895	2.23
<b>OESOPHAGUS WALL</b>		0.0328	
<b>PANCREAS</b>		0.227	2.05
<b>PITUITARY GLAND</b>		0.187	2.76
<b>PROSTATE</b>			
<b>SALIVARY GLANDS</b>		0.166	1.93
<b>SEMINAL VESICLES</b>		0.00300	0.738
<b>SKELETAL MUSCLE</b>		0.0400	0.252
<b>SKIN</b>		0.0500	0.655
<b>SPINAL CORD</b>		0.0241	0.211
<b>SPLEEN</b>		0.617	6.20
<b>STOMACH WALL</b>		0.0481	0.565
<b>TESTIS</b>		0.0260	0.661
<b>THYMUS</b>		0.0710	1.55
<b>THYROID GLAND</b>		0.247	1.13
<b>URINARY BLADDER WALL</b>			
<b>UVEAL TRACT</b>		0.105	0.865

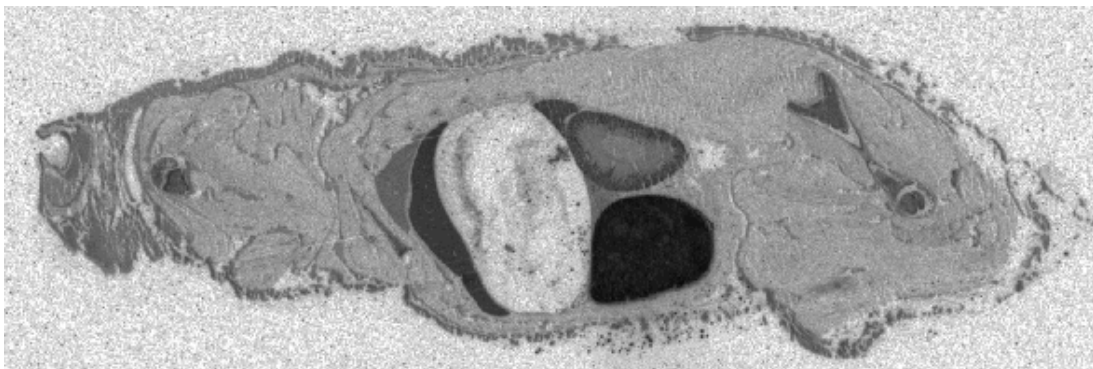
Quantitative tissue distribution of total radioactivity in the male C56 black mouse after single intravenous infusion of various formulations of  $^{14}\text{C}$ -CPTD-1



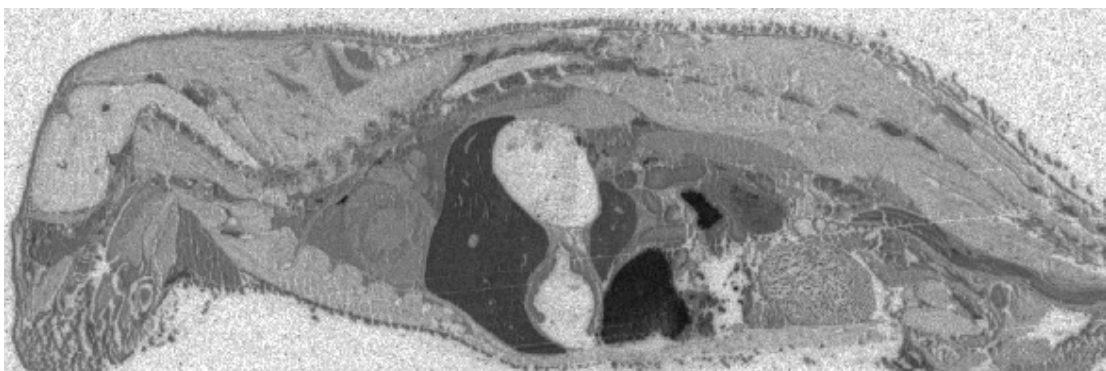
Rat 1 – Section 3 : distribution of radioactivity at 0.17 h (polymerised micelles at 100 mg/4MBq/kg/IV)



Rat 1 – Section 15 : distribution of radioactivity at 0.17 h (polymerised micelles at 100 mg/4MBq/kg/IV)



Rat 2 – Section 2 : distribution of radioactivity at 24 h (polymerised micelles at 100 mg/4MBq/kg/IV)



Rat 2 – Section 14 : distribution of radioactivity at 24 h (polymerised micelles at 100 mg/4MBq/kg/IV)

**TABLE S5:** Tissue distribution of total radioactivity versus time after single intravenous administration of 4 MBq/kg of <sup>14</sup>C-CPTD in non-labeled polymerized micelles and nanosuspension of the free <sup>14</sup>C-CPTD in C57 black male mice

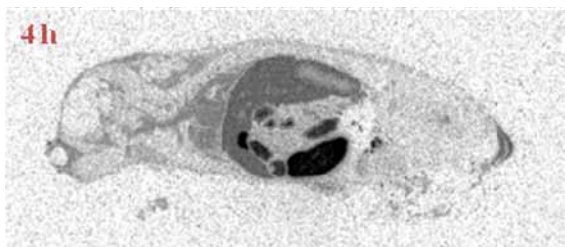
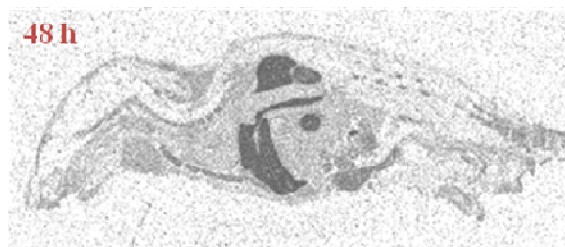
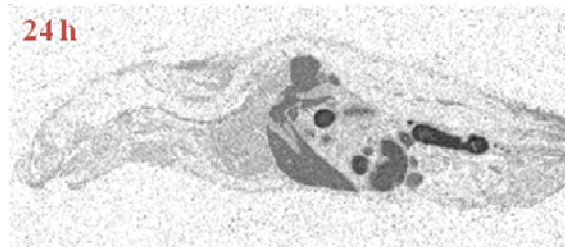
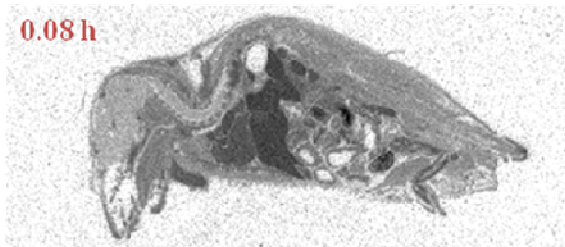
**Tissue distribution (% dose/g)**

Time (h)	Tissues	Adrenal glands	Blood	Bone marrow	Brown fat	Heart	Kidney cortex	Lachrymal gland	Liver	Lungs	Pancreas	Salivary glands	Skeletal muscle	Spleen	Thymus
0.08	Nanosuspension	3.84	2.68	3.98	5.58	7.47	8.86	6.70	50.7	3.86	4.65	3.76	1.43	21.4	1.99
	Micelles	27.8	28.4	7.68	16.1	20.2	36.0	12.4	41.8	21.0	12.7	23.8	2.85	10.5	64.8
1	Nanosuspension	1.32	0.943	0.918	1.42	1.91	3.13	7.27	21.1	1.27	1.62	1.99	BQ(0.6)	3.43	1.32
	Micelles	3.89	7.73	2.95	2.50	3.42	5.68	4.21	9.65	4.68	1.76	3.21	BQ(0.4)	1.91	1.21
4	Nanosuspension	BQ(0.2)	BQ(0.3)	BQ(0.2)	BQ(0.2)	BQ(0.4)	0.665	1.06	2.87	BQ(0.4)	0.628	BQ(0.1)	BQ(0.0)	0.835	BQ(0.0)
	Micelles	3.06	3.46	1.61	1.69	1.98	6.09	1.56	8.05	1.91	BQ(0.8)	0.959	BQ(0.0)	1.94	BQ(0.7)
24	Nanosuspension	BQ(0.0)	BQ(0.1)	BQ(0.0)	BQ(0.0)	BQ(0.0)	BQ(0.0)	BQ(0.0)	BQ(0.2)	BQ(0.0)	BQ(0.0)	BQ(0.0)	BQ(0.0)	BQ(0.0)	BQ(0.0)
	Micelles	1.54	BQ(0.6)	1.04	BQ(0.5)	BQ(0.5)	2.53	BQ(0.3)	4.05	BQ(0.6)	BQ(0.0)	BQ(0.4)	BQ(0.0)	1.45	BQ(0.2)
48	Nanosuspension	BQ(0.0)	BQ(0.0)	BQ(0.0)	BQ(0.0)	BQ(0.0)	BQ(0.0)	BQ(0.0)	BQ(0.4)	BQ(0.0)	BQ(0.0)	BQ(0.0)	BQ(0.2)	BQ(0.0)	BQ(0.0)
	Micelles	1.62	BQ(0.2)	1.54	BQ(0.6)	BQ(0.4)	2.68	BQ(0.6)	4.18	BQ(0.4)	BQ(0.4)	BQ(0.5)	BQ(0.0)	1.41	BQ(0.3)

**T1/2 (h)**

Tissues	Adrenal glands	Blood	Bone marrow	Brown fat	Heart	Kidney cortex	Lachrymal gland	Liver	Lungs	Pancreas	Salivary glands	Skeletal muscle	Spleen	Thymus
Nanosuspension	0.958	10.3	0.898	0.905	0.96	1.11	1.35	7.63	1.39	1.50	0.831	0.000	15.3	0.000
Micelles	37.7	11.4	31.3	23.8	16.5	36.9	12.9	38.6	19.5	25.5	23.1	0.000	95.1	28.3

## Polymerized micelles



## Nanosuspension

